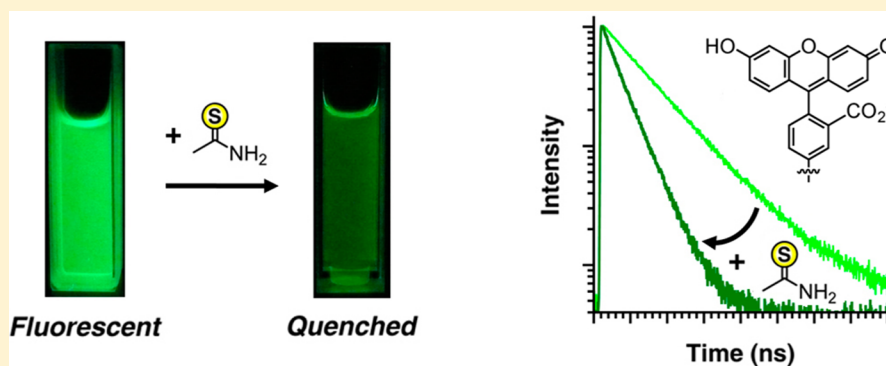


## Thioamide Quenching of Fluorescent Probes through Photoinduced Electron Transfer: Mechanistic Studies and Applications

Jacob M. Goldberg,<sup>†</sup> Solongo Batjargal, Benson S. Chen, and E. James Petersson\*

Department of Chemistry, University of Pennsylvania, Philadelphia, Pennsylvania 19104-6323, United States

## S Supporting Information



**ABSTRACT:** Previously we have shown that thioamides can be incorporated into proteins as minimally perturbing fluorescence-quenching probes to study protein dynamics, folding, and aggregation. Here, we show that the spontaneity of photoinduced electron transfer between a thioamide and an excited fluorophore is governed by the redox potentials of each moiety according to a Rehm–Weller-type model. We have used this model to predict thioamide quenching of various common fluorophores, and we rigorously tested more than a dozen examples. In each case, we found excellent agreement between our theoretical predictions and experimental observations. In this way, we have been able to expand the scope of fluorophores quenched by thioamides to include dyes suitable for microscopy and single-molecule studies, including fluorescein, Alexa Fluor 488, BODIPY FL, and rhodamine 6G. We describe the photochemistry of these systems and explore applications that demonstrate the utility of thioamide quenching of fluorescein to studying protein folding and proteolysis.

Fluorescence quenching experiments can provide valuable information about protein associations, structure, and dynamics.<sup>1–3</sup> These studies often require site-specific incorporation of two spectroscopic labels into the protein of interest.<sup>4,5</sup> Following photoexcitation, energy transfer from one label to the other leads to a change in fluorescence, which is interpreted to extract information about the distance between the probes. Structural information inferred from these distance measurements can be used to generate dynamic models of protein motion or to analyze biological processes.<sup>6,7</sup> Unfortunately, common chromophores tend to be bulky and can disrupt the protein structure if they are arbitrarily introduced into the protein. Smaller reporter pairs that circumvent this problem so that they could be incorporated at almost any position increase the utility of this approach.

Here, we show that a thioamide, which can be prepared as a single-atom substitution in a peptide bond, can be used to develop such a minimalist probe pair by partnering it with one of a variety of fluorophores. This technique is applied in a proof-of-principle experiment as a demonstration of its utility in studying protease activity and monitoring protein folding. We describe mechanistic studies indicating that quenching arises from photoinduced electron transfer and discuss considerations that should be made for selecting an appropriate fluorophore.

Additionally, the model we present should allow investigators to design novel probe pairs using our system by determining whether particular dyes will be quenched by thioamides a priori.

Nonradiative energy transfer can occur through a number of processes that lead to fluorescence quenching. Common mechanisms include Förster resonance energy transfer (FRET), Dexter electron exchange, exciplex formation, and photoinduced electron transfer (PET).<sup>8–12</sup> Unlike FRET and Dexter transfer, which require spectral overlap between the donor and acceptor, PET is governed by redox chemistry and is not inherently restricted to any spectral window.<sup>13</sup> Many PET quenching probes have been identified that operate only over very short distances—e.g., in van der Waals contact with an excited fluorophore—and they have found wide utility in both single-molecule and ensemble studies of nucleic acids or proteins.<sup>14–16</sup> In particular, tryptophan (Trp) and guanine have been employed in these applications since they are easily incorporated and are efficient PET quenchers of several fluorophores, including some boron-dipyrromethene (BODIPY), coumarin, oxazine, and xanthene dyes.<sup>17–19</sup> Unfortunately,

Received: September 22, 2013

Published: November 22, 2013

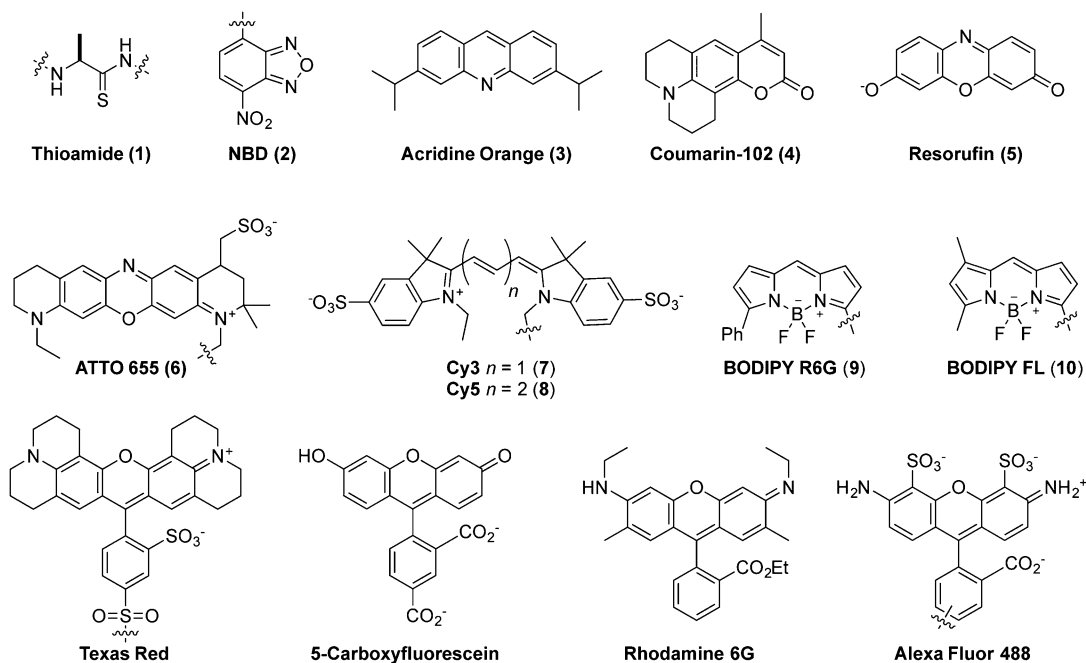


**Figure 1.** Chromophore structures. The chemical structures of a thioamide (e.g., thioalanine, Ala') and fluorophores investigated in this study.

**Table 1.** Thioamide Quenching of Selected Dyes and Their Photophysical and Electrochemical Properties

fluorophore	$\lambda_{\text{ex}}/\lambda_{\text{em}}$ [nm]	$E_{\text{red}}^a$ [V/SCE]	$E_{0,0}^b$ [eV]	$\Delta G_{\text{ET}}^c$ [eV]	$E_Q(\text{SS})^d$ [%]	$\tau^e$ [ns]	$E_Q(\tau)^f$ [%]	volume <sup>g</sup> [Å <sup>3</sup> ]	ref
Coumarin102 (4)	393/487	−2.18	2.85	0.30	0	5.79	0	264	29
NBD <sup>g</sup> (2)	467/538	−0.94	2.47	−0.56	27 ± 1	1.08	19 ± 1	137	30
Alexa Fluor 488 (14)	488/518	−0.635	2.46	−0.86	47 ± 1	4.03	42 ± 1	424	31
5-carboxyfluorescein (12)	492/518	−0.71	2.46	−0.78	44 ± 1	4.04	40 ± 1	346	32
Fluorescein isothiocyanate (16)	492/517				41 ± 1	3.48	36 ± 2		
Fluorescein maleimide (17)	492/516				44 ± 1	3.66	37 ± 2		
Fluorescein click (15)	494/521				44 ± 1	3.95	39 ± 1		
BODIPY FL (10)	502/510	−1.07	2.43	−0.39	61 ± 4	6.13	55 ± 1	258	32
Acridine Orange (3)	502/525	−1.4	2.40	−0.03	3 ± 1	1.83	8 ± 1	305	33
Rhodamine R6G (13)	526/556	−0.95	2.28	−0.36	16 ± 1	3.99	20 ± 1	478	34
BODIPY R6G (9)	528/547	−0.97	2.31	−0.37	45 ± 1	5.28	46 ± 1	305	32
Cy3 (7)	550/570	≤ −1.24	2.21	≥ 0	0	0.22	0	507	32, 35
Resorufin (5)	571/585	−0.47	2.13	−0.69	51 ± 1	2.76	42 ± 1	202	36
Texas Red (11)	582/602	−1.12	2.08	0.01	0	4.23	0	535	32
Cy5 (8)	651/674	−0.88	1.88	−0.03	0	0.97	0	540	37–39
ATTO655 (6)	655/684	−0.42	1.86	−0.47	7 ± 1	2.00	11 ± 1	463	40

<sup>a</sup>Recorded by various methods. <sup>b</sup>Calculated as the average energy of  $\lambda_{\text{ex}}$  and  $\lambda_{\text{em}}$ . <sup>c</sup>Calculated with eq 1. <sup>d</sup>Thioamide quenching efficiencies with standard error calculated as  $E_Q(\text{SS}) = 1 - (F_{\text{Thio}}/F_0)$  where  $F_{\text{Thio}}$  is the fluorescence at  $\lambda_{\text{em}}$  in 50 mM thioacetamide and  $F_0$  is the fluorescence at  $\lambda_{\text{em}}$  in buffer at 298 K. <sup>e</sup>Fluorescence lifetimes of fluorophores in buffer. <sup>f</sup>Thioamide quenching efficiencies with errors estimated from fits calculated as  $E_Q(\tau) = 1 - (\tau_{\text{Thio}}/\tau_0)$  where  $\tau_{\text{Thio}}$  is the fluorescence lifetime in 50 mM thioacetamide and  $\tau_0$  is the fluorescence lifetime in buffer at 298 K. <sup>g</sup>Molecular volume calculated from energy-minimized structures (semiempirical AM1 method) in Spartan (Wavefunction, Inc.).

the general applicability of this technique is somewhat limited by the relatively large size of the quenchers; Trp mutants would be destabilizing at many positions in a protein.

In this respect, thioamide probes (such as 1) are attractive alternatives to conventional PET quenchers. Electrochemically, thioamides ( $E_{\text{ox}} = 0.97$  V vs SCE) are similar to Trp<sup>20</sup> (0.81 V) but substantially different from naturally occurring oxoamides (3.04 V).<sup>21</sup> Many small-molecule fluorescent sensors exploit this difference in oxidation potentials. These sensors often consist of a fluorophore tethered to a thioamide quencher and respond to analyte-induced desulfurization to give an oxoamide with a concomitant gain of fluorescence.<sup>22,23</sup> In a protein context, thioamide bonds are nearly isosteric analogues of

amide bonds,<sup>24</sup> and using semisynthesis techniques, we have recently shown that they can be inserted at almost any position in a sequence with minimal perturbation to the native structure.<sup>25,26</sup> Ultimately, we envision applications in which a fluorophore could be incorporated at a few positions in a protein where it is well-tolerated, and the thioamide bond could be scanned through the backbone to obtain many measurements.

Previously, we have shown that thioamides quench the fluorescence of several aromatic amino acids including *p*-cyanophenylalanine, tyrosine, tryptophan, 7-azatryptophan, 7-methoxycoumarin-4-yl alanine, and acridon-2-yl alanine through FRET or PET mechanisms.<sup>25–27</sup> The small size of

these fluorophores and the relative ease with which they can be genetically incorporated into a protein make them useful tools for a number of applications in studying protein folding or protein–protein interactions. However, the photophysical properties of these probes, particularly their high-energy (i.e., short wavelength) excitation energies and low extinction coefficients, prevent them from being used to study protein dynamics *in vivo* or in single-molecule studies. Here, we report our findings that thioamides quench many fluorophores that are extremely bright and are excited with visible light, including rhodamine 6G (13), BODIPY FL (10), 5-carboxyfluorescein (Fam, 12), and Alexa Fluor 488 (14). We have performed thorough photophysical characterization of Fam, including evaluation of the impact of various common linkers (15–17) used for attachment to proteins and the importance of direct contact with the thioamide for quenching. Finally, we include demonstrations of the application of Fam quenching to monitoring proteolysis with a model trypsin substrate and to tracking the conformation of  $\alpha$ -synuclein ( $\alpha$ S), a protein whose misfolding is implicated in the pathogenesis of Parkinson's disease.

## ■ RESULTS AND DISCUSSION

**Photoinduced Electron Transfer.** The Gibbs free energy of electron transfer ( $\Delta G_{\text{ET}}$ ) from some donor molecule (D) to some acceptor molecule (A) is determined as follows in Rehm–Weller models of electron transfer<sup>28</sup>

$$\Delta G_{\text{ET}} = F\{E_{\text{ox}}(\text{D}) - E_{\text{red}}(\text{A})\} - E_{0,0} + C \quad (1)$$

where  $F$  is the Faraday constant;  $E_{\text{ox}}(\text{D})$  and  $E_{\text{red}}(\text{A})$  are the oxidation and reduction potentials of the electron donor and acceptor molecules, respectively;  $E_{0,0}$  is the zero vibrational electronic excitation energy of the fluorophore, calculated as the average energy of the absorption and emission wavelengths of the fluorescent transition; and  $C$  is a term accounting for Coulombic interactions, which are typically assumed to be negligible in water. The fluorophore can serve as either an electron donor or acceptor, depending on the choice of quencher. In both cases, the spontaneity of electron transfer (the sign of  $\Delta G_{\text{ET}}$ ) can be used to predict whether quenching will occur.

We began our investigation by examining the predictive power of this model. Thioacetamide was taken to be a representative thioamide donor ( $E_{\text{ox}} = 0.97$  V vs SCE<sup>21</sup>), and a variety of common fluorophores (Figure 1) were chosen as acceptors. Using eq 1, we estimated  $\Delta G_{\text{ET}}$  values that spanned  $-0.86$  to  $+0.3$  eV (Table 1). We expected thioamides to quench only those fluorophores for which the sign of  $\Delta G_{\text{ET}}$  is negative. To test these predictions, we recorded the steady-state fluorescence of each fluorophore in three solutions at pH 7.00: 100 mM sodium phosphate (buffer), 50 mM acetamide in buffer, and 50 mM thioacetamide in buffer. By comparing the fluorescence intensities of the buffer and thioacetamide solutions, we determined the quenching efficiencies reported in Table 1 as  $E_{\text{Q}}(\text{SS})$ . Since fluorescence quenching was observed in thioacetamide solutions and not in acetamide solutions, we attribute quenching solely to the thioamide moiety. There was excellent agreement between our theoretical predictions and experimental results.

Several observations from these studies are worth noting. First, the sign of  $\Delta G_{\text{ET}}$  can be used to determine if a particular dye will be quenched, but there is no clear connection between

the magnitude of  $\Delta G_{\text{ET}}$  and  $E_{\text{Q}}$ . This finding is not unexpected, given the complicated nature of excited state dynamics. In principle, a Marcus theory description of the Arrhenius expression could be used to calculate rate constants for PET; however, without detailed knowledge of all of the other photophysical rates,  $E_{\text{Q}}$  values are best determined experimentally. Of course, the efficiency of quenching depends not only on the quenching rate constant but also on the fluorescence lifetime. If the singlet excited state lifetime is longer, quenching can be more efficient, even if  $\Delta G_{\text{ET}}$  is less favorable. For example, BODIPY FL (10), Rhodamine R6G (13), and BODIPY R6G (9) all have nearly identical driving forces but varied quenching that depends on  $\tau$ . Atto655 (6) is quenched less than these dyes, despite having a more negative  $\Delta G_{\text{ET}}$ , due to its short lifetime. Second, care should be taken when interpreting  $\Delta G_{\text{ET}}$  values close to zero. The reported  $E_{\text{red}}$  values for a given fluorophore can vary considerably, especially since different electrochemical techniques for measuring its redox potential can give different results. The cyanine dyes are a convenient example. Lenhard examined 46 of these dyes with phase-selective second-harmonic alternating current voltammetry and found redox potentials that differed nonsystematically by an average of 32 mV from literature values determined by other methods.<sup>41</sup> Although we were unable to find an exact value for the reduction potential of Cy3 (7), some estimates suggest that it is at least below  $-1.24$  V (vs SCE), which corresponds to  $\Delta G_{\text{ET}} \geq 0$  and is consistent with the observation that thioamides do not quench Cy3.<sup>35,38</sup> Third, although we calculated  $\Delta G_{\text{ET}} = -0.03$  eV for Cy5 (8), no quenching was observed. It may be possible to assign this discrepancy to uncertainty in the reported reduction potential, for which literature values span a range of at least 40 mV,<sup>38,39</sup> but it is also reasonable to attribute the difference to approximations inherent in our treatment of the Rehm–Weller model, specifically with respect to Coulombic and solvent effects.<sup>29</sup> Finally, it is important to emphasize that even though we were able to use this model to successfully predict thioamide quenching assuming the thioamide to be the electron donor and the dye to be the electron acceptor it is possible that the roles are reversed for some of the dyes. Further work, such as direct observation of transient radicals, is necessary to determine the direction of PET.

**Mechanistic Studies.** We conducted additional experiments to determine the nature of the quenching mechanism, particularly whether these results were the consequence of dynamic or static processes. In a purely dynamic PET quenching mechanism, the quencher interacts with an excited-state molecule but does not affect molecules remaining in the ground state. Reductions in the steady-state fluorescence intensity arise from the decreased time the fluorophore spends in excited states and from the addition of new nonradiative decay pathways. These phenomena result in shortened fluorescence lifetimes. This is not the case for static quenching, wherein the quencher forms a nonemissive ground-state complex with the fluorophore but does not affect excited molecules. The steady-state fluorescence intensity is attenuated since fewer molecules are excited upon irradiation; however, the fluorescence lifetimes of those molecules that are excited remain unchanged. Since the two quenching mechanisms can be readily distinguished by their effects on fluorescence lifetimes, we used time-correlated, single-photon counting (TCSPC) spectroscopy to measure the lifetime of each sample. We calculated time-resolved quenching efficiencies, listed as

$E_Q(\tau)$  in Table 1, by comparing the average lifetime of each fluorophore in the presence and absence of thioacetamide. These results agree very well with those we obtained for  $E_Q(SS)$ . In all cases where we observed a reduction in steady-state fluorescence intensity, we found corresponding decreases in fluorescence lifetimes consistent with a dynamic quenching mechanism. Furthermore, we found no evidence for the formation of ground-state complexes in the absorption spectra of dilute or concentrated solutions of each fluorophore in all three solvents (see Supporting Information, Figures S2–S17).

To determine if any static component might also contribute to the quenching mechanism, we conducted Stern–Volmer experiments with Fam. We recorded the steady-state and time-resolved fluorescence of Fam in buffered solutions ranging in thioacetamide concentration from 0 to 65 mM. To analyze the dynamic quenching process, we fit our TCSPC data to a linear model with a Stern–Volmer constant  $K_{SV,\tau} = 13.36 \pm 0.04 \text{ M}^{-1}$  (Figure 2). We used this value to calculate a quenching rate

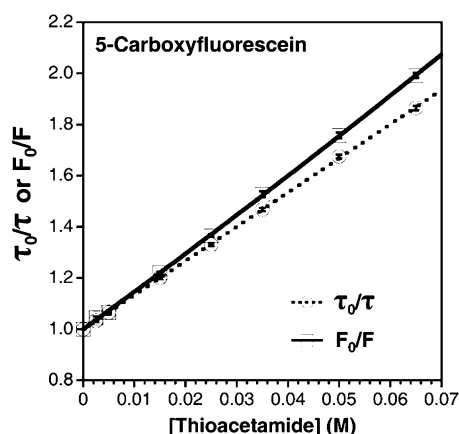


**Figure 2.** Thioacetamide quenching of 5-carboxyfluorescein. Steady-state (solid trace) and time-resolved (dotted trace) Stern–Volmer plots of thioacetamide quenching 5-carboxyfluorescein in 100 mM phosphate buffer, pH 7.00, at 298 K. Steady-state data are fit to quadratic models, and time-resolved data are fit to linear models as described in the text. Error bars are standard error or estimated from fits.

constant,  $k_Q = 3.31 \pm 0.01 \times 10^9 \text{ M}^{-1} \text{ s}^{-1}$ . This value compares favorably to the prediction of the Smoluchowski equation for a diffusion-limited process in which bimolecular collisions result in quenching:  $k_2 = 8.2 \times 10^9 \text{ M}^{-1} \text{ s}^{-1}$ . The discrepancy in  $k_Q$  and  $k_2$  can be attributed to a quenching efficiency factor ( $f_Q$ ) of 0.40 that accounts for the fact that not all collisions are productive but could also simply result from the coarse nature of the model.

The steady-state data were fit to linear and quadratic Stern–Volmer models as described in the Supporting Information. We found superior fits for the quadratic model, which incorporated both dynamic ( $K_D$ ) and static ( $K_S$ ) components:  $K_D = 13.68 \pm 0.51 \text{ M}^{-1}$  and  $K_S = 0.84 \pm 0.31 \text{ M}^{-1}$  (Figure 2). The dynamic component was nearly the same as that determined from TCSPC measurements, and the static component was minimal. Taken together, these findings suggest that thioamide quenching arises almost exclusively from a dynamic mechanism. We have performed a similar analysis of Alexa Fluor 488 and found that thioamide quenching also occurs primarily through dynamic electron transfer (see Supporting Information, Figure S20).

In practical terms, quenching is likely to require transient contact between the thioamide and the fluorophore. To test this hypothesis, we synthesized several short peptides containing a C-terminal Cys labeled with Fam-maleimide (Fam-Cys or  $\psi$ , 17) and either leucine or thioleucine (denoted Leu' or L') at the N-terminus separated by Pro-Pro ( $P_2$ ), Gly-Gly ( $G_2$ ), Pro-Pro-Pro ( $P_3$ ), or Gly-Gly-Gly ( $G_3$ ) spacers. We did not observe quenching in the thioamide  $P_2$ ,  $G_2$ , or  $P_3$  peptides relative to the corresponding oxoamide peptides, but we saw a small amount of quenching in the  $G_3$  peptides ( $6 \pm 0.4\%$ ). The chief difference between the  $P_3$  and  $G_3$  peptides is the flexibility of the peptide spacer, and so we interpret these results to mean contact between the thioamide and fluorophore is necessary for quenching to occur (Figure 3). Since no

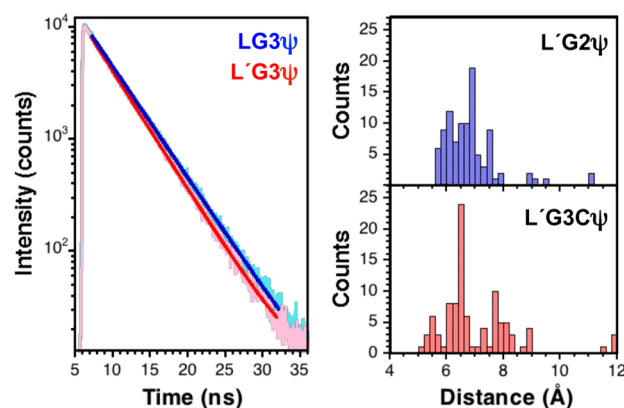


**Figure 3.** Quenching in glycine peptides. Left: Fluorescence lifetime measurements of fluorescein-labeled peptides. Single-exponential fits of fluorescence lifetime measurements of LG3 $\psi$  and L'G3 $\psi$ . Right: Histograms showing the distribution of C1–C2 distances in the conformer ensembles generated from Monte Carlo simulations. See Supporting Information for descriptions of simulations.

quenching was observed in the  $P_2$  or  $G_2$  peptides, proximity alone seems to be insufficient. Analysis of the ensembles of conformations generated using Monte Carlo computational methods for all four peptide scaffolds supports this conclusion since increased fluorophore–thioamide contact is observed in the  $G_3$  peptide relative to the others (see Supporting Information, Figures S23–S25).

**Linker Studies.** Since all of these fluorophores are typically attached to a protein through post-translational covalent modification, we examined the effect of various chemical linkers on quenching. We selected fluorescein as a representative fluorophore and covalently attached it to 6-hexanoic acid, glycine, and cysteine through azide–alkyne (Fam-Click, 15), isothiocyanate (FITC, 16), and maleimide (Fam-Cys,  $\psi$ , 17) chemistries, respectively. Our findings are summarized in Table 1. We observed that the choice of linker had minor effects on the electronic structure of the fluorophore as judged by its spectral properties. The wavelengths of maximum emission or absorption for each conjugate changed by no more than 3 nm relative to that of the parent Fam.

The lifetime decays of free Fam ( $\tau = 4.04 \pm 0.01 \text{ ns}$ ) and Fam-Click ( $\tau = 3.95 \pm 0.01 \text{ ns}$ ) could be fit using a single-exponential function. There was a  $44 \pm 1\%$  reduction of the steady-state fluorescence and a  $40 \pm 1\%$  decrease in the fluorescence lifetimes of both dyes in the presence of 50 mM thioacetamide. On the other hand, FITC and Fam-Cys required biexponential models for satisfactory fits. For Fam-Cys we



found  $\tau_1 = 3.78 \pm 0.02$  ns (87.9% by amplitude; 95.5% by intensity) and  $\tau_2 = 1.29 \pm 0.14$  ns (12.1% by amplitude; 4.5% by intensity) in buffer. In the presence of 50 mM thioacetamide, we found  $\tau_1 = 2.58 \pm 0.01$  ns (63.5% by amplitude; 76.3% by intensity) and  $\tau_2 = 1.39 \pm 0.03$  ns (36.5% by amplitude; 23.7% by intensity). Although the long-lifetime component  $\tau_1$  is unambiguously quenched by thioacetamide, given the errors associated with  $\tau_2$ , it is difficult to determine if the short component is also quenched, though its relative contribution increases considerably. When computed using the average lifetime ( $\tau_{\text{avg}}$ ), Fam-Cys  $E_Q(\tau)$  is essentially the same as Fam-Click  $E_Q(\tau)$  ( $37 \pm 2\%$ ). Fam-Cys steady-state quenching is also the same:  $E_Q(\text{SS}) = 44 \pm 1\%$ .

Thioacetamide quenching was slightly less efficient for FITC with  $E_Q(\tau) = 36 \pm 2\%$  and  $E_Q(\text{SS}) = 41 \pm 1\%$ . Specifically, we found long ( $\tau_1 = 3.67 \pm 0.02$  ns; 81% by amplitude, 92% by intensity) and short ( $\tau_2 = 1.32 \pm 0.09$  ns; 19% by amplitude, 8% by intensity) lifetime components that accounted for the observed decay trace in buffer. Both components were quenched by 50 mM thioacetamide ( $\tau_1 = 2.38 \pm 0.01$  ns; 75.8% by amplitude, 88.6% by intensity and  $\tau_2 = 0.96 \pm 0.05$  ns; 24.2% by amplitude, 11.4% by intensity). Previous reports have shown that FITC adducts have lower quantum yields than other fluorescein adducts, and indeed, the intensity-weighted average lifetime of the conjugate in buffer ( $\tau_{\text{avg}} = 3.48 \pm 0.08$  ns) was roughly 15% less than that of Fam.<sup>42</sup> We attribute this difference, not observed for the other conjugates, to the linker. Upon reaction with amines, isothiocyanates produce thioureas, which are chemically similar to thioamides. We speculated that the thiourea functional group might act as an intramolecular quencher and attenuate the fluorescence of fluorescein. To test this hypothesis, we measured the fluorescence of Fam in buffered solutions of 50 mM urea and 50 mM thiourea. Although we observed no difference in the spectral properties in either solution relative to those of Fam in buffer, we found thiourea to have the same steady-state fluorescence quenching efficiency ( $45 \pm 1\%$ ) as thioacetamide. In spite of the inherent quenching due to the thiourea linker in FITC adducts, these labels can still be used in thioamide quenching probe pairs.

**Monitoring Protease Activity.** We applied these lessons to the design of profluorescent substrates for monitoring protease activity in real time. The strategy, which is illustrated in Figure 4, employs a short peptide that is labeled with a thioamide and fluorophore on opposite ends such that its fluorescence is quenched. When the intervening amino acid sequence is recognized by a proteolytic enzyme, the peptide is cleaved, allowing the fluorophore and thioamide to diffuse away from each other with a concomitant gain of fluorescence. We used this approach in a proof-of-principle experiment to examine the proteolysis of the short peptide A'AFKG $\psi$  by trypsin (A' represents thioalanine,  $\psi$  represents Fam-Cys). Upon addition of trypsin to a 1.4  $\mu\text{M}$  solution of the peptide, we observed an increase in fluorescence at a rate ( $\sim 0.1 \mu\text{M}/\text{min}$  over the first 5 min) falling in the middle of the very broad range of previous measurements of trypsin kinetics with canonical small peptide substrates ( $3.5 \times 10^{-5}$ – $50 \mu\text{M}/\text{min}$  under the conditions of our experiment, see Supporting Information, Table S2).<sup>43–45</sup> In the absence of protease, the thiopeptide fluorescence remained nearly constant. The fluorescence of the corresponding oxoamide peptide (AAFKG $\psi$ ) was constant in the presence and absence of protease, showing that the changes observed with A'AFKG $\psi$

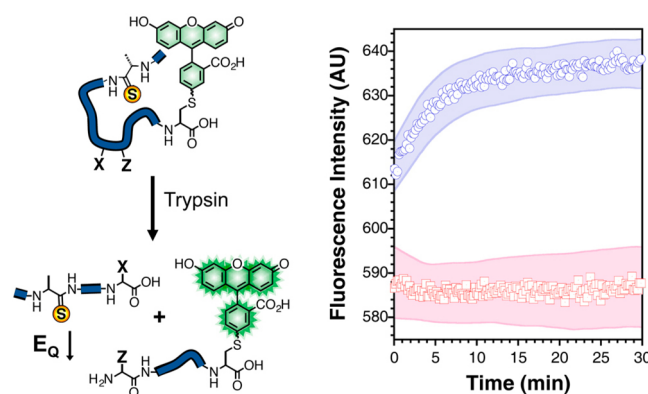


**Figure 4.** Protease activity. Left: A cartoon illustrating the cleavage of a profluorescent peptide substrate by a protease as described in the text. Right: Fluorescence of 1.4  $\mu\text{M}$  A'AFKG $\psi$  peptide in the presence (blue circles) and absence (red squares) of 250  $\mu\text{g}/\text{mL}$  of trypsin in 67 mM sodium phosphate buffer, pH 7.6. Excitation was at 494 nm, and emission was monitored at 522 nm. Shaded areas represent standard error as calculated from at least three independent trials.

could be exclusively attributed to thioalanine quenching of Fam (see Supporting Information, Figure S26).

As the range of trypsin data exemplifies, enzyme kinetics can vary enormously with substrate structure.<sup>46</sup> We believe that small thioamide probes will allow investigators to obtain Michaelis–Menten parameters that more accurately reflect those of native substrates than larger fluorophore–quencher pairs. We are currently investigating the scope of this method with several classes of proteases and in a variety of matrices, including cell lysate.

**Monitoring Protein Folding.** We have also applied the Fam/thioamide probe pair to monitoring the refolding of an intrinsically disordered protein,  $\alpha\text{S}$ . The aggregation of  $\alpha\text{S}$ , which is believed to underlie Parkinson's disease pathology, occurs by formation of soluble  $\beta$ -sheet-rich oligomers that eventually convert into larger, insoluble fibrils.<sup>47</sup> Understanding the structural dynamics of the metastable  $\alpha\text{S}$  monomers may help to explain what primes  $\alpha\text{S}$  for oligomerization and subsequent fibrillization.<sup>48</sup> We have previously shown that we can monitor conformational changes in monomeric  $\alpha\text{S}$ , using urea or trimethylamine oxide (TMAO) to denature or compact  $\alpha\text{S}$ , respectively.<sup>26,49</sup> These experiments used *p*-cyanophenylalanine (Cnf) and thioamide labels to track the distances between pairs of residues in the 8–30 Å range over which this FRET probe pair is useful.<sup>27</sup> Our studies complemented similar studies by Deniz and co-workers using longer-range FRET pairs.<sup>50</sup> We can use Fam/thioamide pairs to observe short distance interactions that are not resolvable by Cnf/thioamide pairs. Moreover, Fam/thioamide studies can be performed with very dilute solutions or in complex mixtures for which the UV range excitation of Cnf would result in high levels of background fluorescence.

In a proof-of-principle experiment, we have examined  $\alpha\text{S}$  constructs labeled with Fam at position 114 or 125 and with a thioglutamate at position 130 or 137 ( $\alpha\text{S}_{\psi_{114}\text{E}'_{137}}$  or  $\alpha\text{S}_{\psi_{125}\text{E}'_{130}}$ ) (Figure 5). Oxoamide control experiments ( $\alpha\text{S}_{\psi_{114}}$  or  $\alpha\text{S}_{\psi_{125}}$ ) were essential to proper data interpretation. Fam fluorescence in the oxoamide proteins is quenched by the addition of 4 M TMAO, which could lead to an overestimation of thioamide quenching without appropriate correction (see Supporting Information, Figures S37–S39). To minimize the

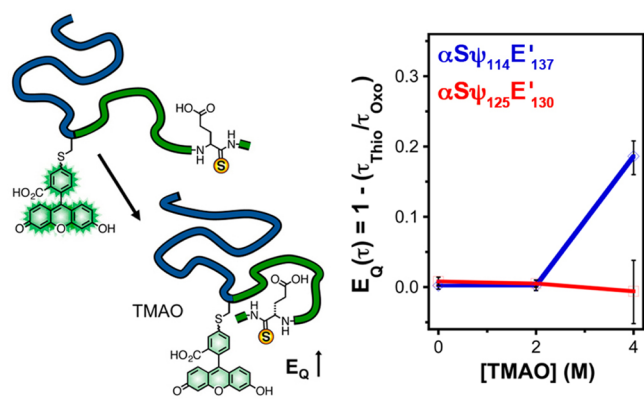


**Figure 5.** Refolding assay. Left: Monomeric double-labeled  $\alpha$ S is mixed with TMAO to induce compaction and an increase in quenching efficiency, determined from TCSPC measurements ( $E_Q(\tau) = 1 - \tau_{\text{Thio}}/\tau_{\text{Oxo}}$ ). Right:  $E_Q(\tau)$  of  $\alpha$ S $\psi_{114}E'_{137}$  (blue) or  $\alpha$ S $\psi_{125}E'_{130}$  (red) determined at varying concentrations of TMAO. Error bars represent the uncertainty in the fitted average lifetime values for each condition. Fits to raw TCSPC data are shown in the Supporting Information.

influence of concentration matching on measurements of quenching efficiency, we determined  $E_Q(\tau)$  values for the labeled  $\alpha$ S constructs in varying TMAO concentrations by performing TCSPC experiments.

In 0 M TMAO, no thioamide-specific quenching was observed for either set of constructs. This indicates that there is no contact between the Fam labels and the thioamides prior to TMAO addition. Little change in  $E_Q(\tau)$  was observed in 2 M TMAO; however, upon further compaction in 4 M TMAO, substantial quenching ( $E_Q(\tau) = 19\%$ ) was observed for  $\alpha$ S $\psi_{114}E'_{137}$ , while no quenching ( $E_Q(\tau) = 0\%$ ) was observed for  $\alpha$ S $\psi_{125}E'_{130}$ . This implies that during compaction the C-terminal tail of  $\alpha$ S folds back on the 114 region but that positions 125 and 130 are not oriented properly for quenching, despite their proximity in the amino acid sequence. These experiments show that Fam quenching by thioamides can be used to observe changes in interactions between regions of a protein during a conformational change. Since near van der Waals contact is required, one can interpret positive thioamide quenching results as showing direct contact between two residues in the protein sequence. Unlike our Cnf experiments, where one could observe a decrease in interchromophore distance in lower concentrations of TMAO, no change in quenching is observed in 2 M TMAO here.<sup>26</sup> This indicates that sufficient compaction to bring the 114 region into contact with Glu<sub>137</sub> only occurs in 4 M TMAO. If this probe system can successfully be applied at the single-molecule level, it will nicely complement fluorophore pairs such as fluorescein and rhodamine that cannot provide highly local contact information.

## CONCLUSIONS

In summary, we have shown that the free energy of electron transfer can be successfully used to predict whether thioamides quench various fluorophores through photoinduced electron transfer, including dyes suitable for microscopy and single-molecule studies, such as fluorescein, Alexa Fluor 488, BODIPY FL, and rhodamine 6G. We have described the photochemistry of these systems and in the case of fluorescein, analyzed the impact of common linkers used to attach these dyes to proteins.

We have also explored preliminary applications demonstrating the utility of thioamide quenching to studying proteolysis and the folding of an intrinsically disordered protein. Attempts to extend the protease results to applications with cultured cells and the  $\alpha$ S results to single-molecule fluorescence correlation spectroscopy (FCS) experiments are underway.

## METHODS

**Small-Molecule Fluorescence Spectroscopy.** Fluorescence measurements in the presence and absence of 50 mM acetamide or 50 mM thioacetamide were conducted for each fluorophore in 100 mM sodium phosphate buffer, pH 7.00. Concentrated stocks of each fluorophore in buffer were prepared immediately prior to use, with the exception of Alexa Fluor 488, BODIPY FL, BODIPY R6G, Cy3, and Cy5. Concentrated stocks of these dyes were prepared one day prior to use to allow the succinimidyl esters to hydrolyze. Spectroscopic grade ethanol was added to the BODIPY R6G sample to aid in dissolution. NBD and fluorescein conjugates were prepared as described in the Supporting Information. For each fluorophore, samples were prepared by diluting the concentrated stock with additional buffer and 100 mM solutions of acetamide or thioacetamide in buffer such that all solutions of a given fluorophore were equimolar. Steady-state fluorescence spectra were collected as the average of three scans at 25 °C of three samples of each solution using a Cary Eclipse fluorometer (currently Agilent Technologies). Excitation wavelengths are given in the Supporting Information. The  $E_Q$  values reported in Table 1 are the average of three trials.

**Small-Molecule Fluorescence Lifetime Measurements.** Time-resolved fluorescence measurements were performed on freshly prepared samples using the time-correlated single photon counting (TCSPC) method. The TCSPC system consisted of a blue diode laser generating 10 MHz output pulses at 405 nm, a subtractive double monochromator with an MCP-PMT, and a TCSPC computer board. Emission was monitored at the wavelength of maximum fluorescence. Data analysis was performed with FluoFit software (Picoquant) using an exponential decay model as described in the Supporting Information.

**Small-Molecule Absorbance Spectroscopy.** UV–visible spectra were acquired of dilute and concentrated solutions of each fluorophore in 100 mM sodium phosphate buffer, pH 7.00; in 50 mM thioacetamide; and in 50 mM acetamide in quartz cells with 1.00 cm path lengths. Representative spectra are shown in the Supporting Information.

**Molecular Volume Calculations.** The ground-state geometries of each fluorophore were optimized at the AM1 level, and the molecular volume was calculated using Spartan (Wavefunction, Inc.). Reactive handles were not included in these calculations.

**Thiourea Quenching of 5-Carboxyfluorescein.** The quenching efficiency of thiourea was determined by comparing the fluorescence of Fam in the presence and absence of thiourea or urea. A concentrated stock of Fam in 100 mM sodium phosphate buffer, pH 7.00, was used to prepare solutions that were 1.6  $\mu$ M fluorophore in pure buffer, 50 mM thiourea and buffer, or 50 mM urea and buffer. Fluorescence spectra of each sample were acquired in triplicate at 25 °C using the same parameters described above for the thioacetamide experiments.

**Stern–Volmer Experiments.** Concentrated stock solutions of Fam or A488 in 100 mM sodium phosphate buffer, pH 7.00, were diluted with 100 mM thioacetamide and buffer to prepare samples of uniform dye concentration and variable thioacetamide concentration (0, 2.5, 5, 15, 25, 35, 50, and 65 mM). The Fam solutions were excited at 492 nm, and emission was recorded from 500 to 600 nm. The A488 solutions were excited at 475 nm, and emission was recorded from 485 to 600 nm. For all steady-state measurements, the excitation and emission slit widths were 5 nm; the scan rate was 120 nm/min; the data pitch was 1.0 nm; and the averaging time was 0.1 s. Measurements were made in 1.00 cm quartz cuvettes at 25 °C. For Fam, the fluorescence intensity at 522 nm was averaged from three separate trials to obtain values for Stern–Volmer calculations. The

fluorescence intensity at 516 nm from three separate trials was averaged to obtain values for Stern–Volmer calculations for the A488 samples. A thorough description of the data analysis can be found in the Supporting Information.

**Peptide Synthesis.** Peptides were synthesized on solid phase using standard Fmoc chemistry and purified to homogeneity by reverse-phase high performance liquid chromatography (HPLC). Thioamide benzotriazole precursors were either commercially available or synthesized according to literature precedent. Explicit protocols are provided in the Supporting Information.

**Protease Experiments.** A sample of trypsin type II from porcine pancreas was dissolved in cold 1 mM hydrochloric acid at a concentration of 2.5 mg/mL. Concentrated stocks of AAFKG $\psi$  and A'AFKG $\psi$  peptides in 67 mM sodium phosphate buffer, pH 7.6, were prepared and cooled on ice. Samples were prepared in triplicate immediately before fluorescence measurements were taken such that the final concentration of peptide was approximately 1.4  $\mu$ M and the final concentration of trypsin was 250  $\mu$ g/mL. Samples of equimolar peptide in an equivalent HCl/buffer solution in the absence of enzyme were used as controls. The fluorescence of each sample was measured over the course of 45 min with the kinetics module of a Varian Cary Eclipse fluorescence spectrophotometer fitted with a Peltier multicell holder. The excitation wavelength was 494 nm, and the emission wavelength was 522 nm.

**Protein Semisynthesis.** Thioamide-labeled  $\alpha$ S constructs were synthesized by ligation of an expressed protein fragment corresponding to  $\alpha$ S<sub>1–113</sub> or  $\alpha$ S<sub>1–124</sub> as intein fusions. After ligation to the corresponding thiopeptide,  $\alpha$ S<sub>114–140</sub>C<sub>114</sub>E'<sub>137</sub> or  $\alpha$ S<sub>125–140</sub>C<sub>125</sub>E'<sub>130</sub>, the protein was labeled with fluorescein-maleimide and purified by fast protein liquid chromatography (FPLC), followed by HPLC. Full descriptions of protein synthesis and characterization are given in the Supporting Information.

**$\alpha$ S Refolding Experiments.** Tris buffers (20 mM Tris, 100 mM NaCl, pH 7.5) containing trimethylamine oxide (TMAO) were prepared such that upon addition of protein (absorbance of final solution at 492 nm was between 0.11 and 0.07, corresponding to 1.47–1.07  $\mu$ M) the final TMAO concentrations were 0, 2, and 4 M. Fluorescence lifetimes were measured immediately following sample dilution in TMAO (to a final volume of 125  $\mu$ L) using a Photon Technologies International (PTI) Quantamaster 40 with a 486 nm pulsed light-emitting diode (LED) light source using time-correlated single photon counting (TCSPC) detection. Full details are given in the Supporting Information.

## ■ ASSOCIATED CONTENT

### ■ Supporting Information

Materials, detailed descriptions of all experimental procedures, calculations, and representative spectral data, their associated fits, and residuals. This material is available free of charge via the Internet at <http://pubs.acs.org>.

## ■ AUTHOR INFORMATION

### Corresponding Author

ejpetersson@sas.upenn.edu

### Present Address

<sup>†</sup>Department of Chemistry, Massachusetts Institute of Technology, Cambridge, MA 02139, United States.

### Notes

The authors declare no competing financial interest.

## ■ ACKNOWLEDGMENTS

This work was supported by funding from the University of Pennsylvania, the Alfred P. Sloan Foundation (BR2012-085 to E.J.P.), the National Science Foundation (NSF CHE-1150351 to E.J.P.), and the National Institutes of Health (NIH NS081033 to E.J.P.). We thank Rakesh Kohli for assistance

with HRMS (supported by NIH RR-023444) and MALDI-MS (supported by NSF MRI-0820996). We thank Jeff Saven for use of the fluorometer, and we are grateful to Tom Troxler for assistance with the TCSPC measurements collected at the Ultrafast Optical Processes Laboratory at the University of Pennsylvania (supported by NIH P41GM104605). J.M.G. thanks the University of Pennsylvania for a dissertation completion fellowship and Xing Chen for assistance with peptide synthesis. S.B. thanks the Parkinson's Disease Foundation for a summer fellowship. B.S.C. thanks the Penn Undergraduate Research Mentorship program for funding.

## ■ REFERENCES

- (1) Eftink, M. R. *Methods Biochem. Anal.* **1991**, *35*, 127–205.
- (2) Royer, C. A. *Chem. Rev.* **2006**, *106*, 1769–1784.
- (3) Weiss, S. *Nat. Struct. Biol.* **2000**, *7*, 724–729.
- (4) Sinkeldam, R. W.; Greco, N. J.; Tor, Y. *Chem. Rev.* **2010**, *110*, 2579–2619.
- (5) Ha, T.; Ting, A. Y.; Liang, J.; Caldwell, W. B.; Deniz, A. A.; Chemla, D. S.; Schultz, P. G.; Weiss, S. *Proc. Natl. Acad. Sci. U.S.A.* **1999**, *96*, 893–898.
- (6) Lavis, L. D.; Raines, R. T. *ACS Chem. Biol.* **2008**, *3*, 142–155.
- (7) Taraska, J. W. *Curr. Opin. Struct. Biol.* **2012**, *22*, 507–513.
- (8) Dexter, D. L. *J. Chem. Phys.* **1953**, *21*, 836–850.
- (9) Forster, T. *Discuss. Faraday Soc.* **1959**, No. 27, 7–17.
- (10) Gould, I. R.; Young, R. H.; Mueller, L. J.; Farid, S. *J. Am. Chem. Soc.* **1994**, *116*, 8176–8187.
- (11) Benelli, T.; Tomasulo, M.; Raymo, F. M. In *Molecular Switches*; Wiley-VCH Verlag GmbH & Co. KGaA: New York, 2011; pp 697–717.
- (12) Hurenkamp, J. H.; de Jong, J. J. D.; Browne, W. R.; van Esch, J. H.; Feringa, B. L. *Org. Biomol. Chem.* **2008**, *6*, 1268–1277.
- (13) Ueno, T.; Urano, Y.; Setsukinai, K.-i.; Takakusa, H.; Kojima, H.; Kikuchi, K.; Ohkubo, K.; Fukuzumi, S.; Nagano, T. *J. Am. Chem. Soc.* **2004**, *126*, 14079–14085.
- (14) Hudgins, R. R.; Huang, F.; Gramlich, G.; Nau, W. M. *J. Am. Chem. Soc.* **2002**, *124*, 556–564.
- (15) Crisalli, P.; Hernandez, A. R.; Kool, E. T. *Bioconjugate Chem.* **2012**, *23*, 1969–1980.
- (16) Schuler, B.; Hofmann, H. *Curr. Opin. Struct. Biol.* **2013**, *23*, 36–47.
- (17) Togashi, D. M.; Szczupak, B.; Ryder, A. G.; Calvet, A.; O'Loughlin, M. J. *Phys. Chem. A* **2009**, *113*, 2757–2767.
- (18) Doose, S.; Neuweiler, H.; Sauer, M. *ChemPhysChem* **2009**, *10*, 1389–1398.
- (19) Sun, Q. F.; Lu, R.; Yu, A. C. *J. Phys. Chem. B* **2012**, *116*, 660–666.
- (20) DeFelippis, M. R.; Murthy, C. P.; Faraggi, M.; Klapper, M. H. *Biochemistry* **1989**, *28*, 4847–4853.
- (21) Bordwell, F. G.; Algrim, D. J.; Harrelson, J. A., Jr. *J. Am. Chem. Soc.* **1988**, *110*, 5903–5904.
- (22) Chae, M. Y.; Czarnik, A. W. *J. Am. Chem. Soc.* **1992**, *114*, 9704–9705.
- (23) Song, K. C.; Kim, J. S.; Park, S. M.; Chung, K.-C.; Ahn, S.; Chang, S.-K. *Org. Lett.* **2006**, *8*, 3413–3416.
- (24) Choudhary, A.; Raines, R. T. *ChemBioChem* **2011**, *12*, 1801–1807.
- (25) Batjargal, S.; Wang, Y. J.; Goldberg, J. M.; Wissner, R. F.; Petersson, E. J. *J. Am. Chem. Soc.* **2012**, *134*, 9172–9182.
- (26) Wissner, R. F.; Batjargal, S.; Fadzen, C. M.; Petersson, E. J. *J. Am. Chem. Soc.* **2013**, *135*, 6529–6540.
- (27) Goldberg, J. M.; Batjargal, S.; Petersson, E. J. *J. Am. Chem. Soc.* **2010**, *132*, 14718–14720.
- (28) Rehm, D.; Weller, A. *Isr. J. Chem.* **1970**, *8*, 259–271.
- (29) Seidel, C. A. M.; Schulz, A.; Sauer, M. H. M. *J. Phys. Chem.* **1996**, *100*, 5541–5553.
- (30) Xu, Z.; Kim, G.-H.; Han, S. J.; Jou, M. J.; Lee, C.; Shin, I.; Yoon, J. *Tetrahedron* **2009**, *65*, 2307–2312.



- (31) Chen, H.; Ahsan, S. S.; Santiago-Berrios, M. E. B.; Abruna, H. D.; Webb, W. W. *J. Am. Chem. Soc.* **2010**, *132*, 7244–7245.
- (32) Torimura, M.; Kurata, S.; Yamada, K.; Yokomaku, T.; Kamagata, Y.; Kanagawa, T.; Kurane, R. *Anal. Sci.* **2001**, *17*, 155–160.
- (33) Guha, S. N.; Mittal, J. P. *J. Photochem. Photobiol.* **1995**, *92*, 181–188.
- (34) Sauer, M.; Han, K. T.; Müller, R.; Nord, S.; Schulz, A.; Seeger, S.; Wolfrum, J.; Arden-Jacob, J.; Deltau, G.; Marx, N. J.; Zander, C.; Drexhage, K. H. *J. Fluoresc.* **1995**, *5*, 247–261.
- (35) Sanborn, M. E.; Connolly, B. K.; Gurunathan, K.; Levitus, M. *J. Phys. Chem. B* **2007**, *111*, 11064–11074.
- (36) Çakir, S.; Arslan, E. *Chem. Pap.* **2010**, *64*, 386–394.
- (37) Vogelsang, J.; Kasper, R.; Steinhauer, C.; Person, B.; Heilemann, M.; Sauer, M.; Tinnefeld, P. *Angew. Chem., Int. Ed.* **2008**, *47*, 5465–5469.
- (38) Stein, I. H.; Capone, S.; Smit, J. H.; Baumann, F.; Cordes, T.; Tinnefeld, P. *ChemPhysChem* **2012**, *13*, 931–937.
- (39) Dietrich, A.; Buschmann, V.; Müller, C.; Sauer, M. *Rev. Mol. Biotechnol.* **2002**, *82*, 211–231.
- (40) Vogelsang, J.; Cordes, T.; Forthmann, C.; Steinhauer, C.; Tinnefeld, P. *Proc. Natl. Acad. Sci. U.S.A.* **2009**, *106*, 8107–8112.
- (41) Lenhard, J. *J. Imaging Sci.* **1986**, *30*, 27–35.
- (42) Klonis, N.; Sawyer, W. H. *Photochem. Photobiol.* **2003**, *77*, 502–509.
- (43) Walsh, K. A. *Methods Enzymol.* **1970**, *19*, 41–63.
- (44) Grant, G. A.; Eisen, A. Z. *Biochemistry* **1980**, *19*, 6089–6095.
- (45) Evnin, L. B.; Vasquez, J. R.; Craik, C. S. *Proc. Natl. Acad. Sci. U.S.A.* **1990**, *87*, 6659–6663.
- (46) Lottenberg, R.; Christensen, U.; Jackson, C. M.; Coleman, P. L.; Laszlo, L. *Methods Enzymol.* **1981**, *80*, 341–361.
- (47) Auluck, P. K.; Caraveo, G.; Lindquist, S. *Annu. Rev. Cell Dev. Biol.* **2010**, *26*, 211–233.
- (48) Drescher, M.; Huber, M.; Subramaniam, V. *ChemBioChem* **2012**, *13*, 761–768.
- (49) Wissner, R. F.; Wagner, A. M.; Warner, J. B. *Synlett* **2013**, *24*, 2454–2458.
- (50) Ferreón, A. C. M.; Moosa, M. M.; Gambin, Y.; Deniz, A. A. *Proc. Natl. Acad. Sci. U.S.A.* **2012**, *109*, 17826–17831.